Accepted Manuscript

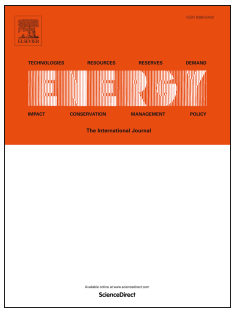

Efficient hydrogen production with CO_2 capture using gas switching reforming

Shareq Mohd Nazir, Jan Hendrik Cloete, Schalk Cloete, Shahriar Amini

PII: S0360-5442(19)31411-2

DOI: https://doi.org/10.1016/j.energy.2019.07.072

Reference: EGY 15742

To appear in: *Energy*

Received Date: 21 January 2019

Revised Date: 3 July 2019

Accepted Date: 10 July 2019

Please cite this article as: Nazir SM, Cloete JH, Cloete S, Amini S, Efficient hydrogen production with CO_2 capture using gas switching reforming, *Energy* (2019), doi: https://doi.org/10.1016/j.energy.2019.07.072.

Efficient hydrogen production with CO_2 capture using gas switching reforming

Shareq Mohd Nazir[a*], Jan Hendrik Cloete[b], Schalk Cloete[b], Shahriar Amini[a,b**]

[a]Department of Energy and Process Engineering, Norwegian University of Science and Technology, Trondheim, Norway

[b]SINTEF Industry, Trondheim, Norway

Abstract

Hydrogen is a promising carbon-neutral energy carrier for a future decarbonized energy sector. This work presents process simulation studies of the gas switching reforming (GSR) process for hydrogen production with integrated CO_2 capture (GSR-H2 process) at a minimal energy penalty. Like the conventional steam methane reforming (SMR) process, GSR combusts the off-gas fuel from the pressure swing adsorption unit to supply heat to the endothermic reforming reactions. However, GSR completes this combustion using the chemical looping combustion mechanism to achieve fuel combustion with CO_2 separation. For this reason, the GSR-H2 plant incurred an energy penalty of only 3.8 %-points relative to the conventional SMR process with 96% CO_2 capture. Further studies showed that the efficiency penalty is reduced to 0.3 %-points by including additional thermal mass in the reactor to maintain a higher reforming temperature, thereby facilitating a lower steam to carbon ratio. GSR reactors are standalone bubbling fluidized beds that will be relatively easy to scale up and operate under pressurized conditions, and the rest of the process layout uses commercially available technologies. The ability to produce clean hydrogen with no energy penalty combined with this inherent scalability makes the GSR-H2 plant a promising candidate for further research.

*Corresponding author 1
Email: shareq.m.nazir@ntnu.no
Telephone: +47- 48654776
Address: Kolbjørn Hejes vei 1b, Varmeteknisk*A514, NTNU, NO-7491 Trondheim, Norway
**Corresponding author 2
Email: shahriar.amini@ntnu.no
Telephone: +47- 46639721
Address: Kolbjørn Hejes vei 1b, Dept. of Energy and Process Engineering, NTNU, NO-7491 Trondheim, Norway

Keywords: Hydrogen production; Gas switching reforming; CO_2 capture; Steam methane reforming; Energy penalty; Chemical looping reforming.

Nomenclature

CA	CO_2 Avoided
CC	CO_2 Capture
CCS	CO_2 Capture and Storage
CLC	Chemical Looping Combustion
CLR	Chemical Looping Reforming
CSTR	Continuous Stirred Tank Reactor
FTR	Fired Tubular Reformer
GSC	Gas Switching Combustion
GSR	Gas Switching Reforming
GSR-H2	Gas Switching Reforming Hydrogen plant
LHV	Lower Heating Value
MDEA	Methyl Diethanolamine
NG	Natural Gas
NGCC	Natural Gas Combined Cycle
PSA	Pressure Swing Adsorption
SMR	Steam Methane Reforming
SPECCA	Specific Primary Energy Consumption for CO_2 Avoided
S/C	Steam to Carbon
TIT	Turbine Inlet Temperature
WGS	Water-Gas Shift

Symbols

η_{H2}	Hydrogen Production Efficiency
$\eta_{eq,H2}$	Equivalent Hydrogen Production Efficiency
E_{CO2}	CO_2 emission intensity from the process
E_{el}	Avoided CO_2 intensity of electricity export/import
$E_{eq,CO2}$	Equivalent CO_2 emission intensity from the process
E_{NG}	CO_2 emission intensity of NG combustion

E_{th}	Avoided CO_2 intensity of thermal energy exports (steam export)
$m_{eq,NG}$	Equivalent mass flow rate of NG
P_1	Pressure of PSA inlet stream
P_2	Pressure of PSA off-gas stream from PSA
Q_{th}	Thermal energy export in the form of 6 bar steam
W_{el}	Net electrical power

1 Introduction

The recent release of the Intergovernmental Panel on Climate Change (IPCC) report on global warming of 1.5 °C [1] has once again emphasized the urgency of reducing global greenhouse gas emissions. Hydrogen offers a versatile solution as a carbon-free energy carrier for industry, transport and power. However, the vast majority of current hydrogen production comes from fossil fuels with large associated CO_2 emissions, mainly steam methane reforming (SMR) [2].

One promising solution for clean hydrogen production is electrolysis using renewable electricity, but thermochemical conversion of fossil fuels remains significantly cheaper than these advanced hydrogen production pathways [3, 4]. The inclusion of CO_2 capture and storage (CCS) in conventional fossil fuel-based hydrogen production processes offers another solution, but the cost increase associated with conventional CCS is high (40-100%) [5].

The primary challenge facing conventional CO_2 capture processes is the large energy penalty that results in large CO_2 avoidance costs. In a conventional SMR based H_2 plant, CO_2 can be captured from the raw hydrogen gas before PSA, tail gas from the PSA or the flue gas from reformer [6]. The cost of CO_2 avoided was estimated to be more than the CO_2 emission tax (that is between 10-20 €/t-CO_2) when 90% CO_2 is captured from the flue gas from the reformer [6]. In another study by Spallina et al. [7], it was reported that the addition of an MDEA CO_2 capture process to the conventional SMR H_2 production process reduced the equivalent H_2 production efficiency from 81% to 67%. Such a substantial drop in efficiency has large negative implications on process economics, leading to a high CO_2 avoidance cost around €100/ton [7]. Cormos et al. [8] compared SMR and auto-thermal reforming (ATR) processes with CO_2 capture to produce pure H_2. The SMR and ATR processes were integrated with gas-liquid absorption system to separate the CO_2, and the H_2-rich gas was further treated in a PSA to produce >99.95% pure H_2. The SMR plant with CO_2 capture is more energy and cost efficient when compared to ATR plant for hydrogen production [8].

Chemical looping reforming (CLR) [9] offers one solution to this challenge by deploying an oxygen carrier material to transport oxygen from air to fuel without the energy penalty usually associated with air separation. However, the conventional CLR process does not offer a natural integration of the pressure swing adsorption (PSA) off-gas fuel to supply the reforming heat as in the conventional SMR process. It has therefore been simulated in a pre-combustion capture configuration using MDEA to capture CO_2 with the H_2-rich off-gas being used as a low-carbon fuel for power production [10].

The integration of membranes into the CLR process can achieve hydrogen production without any energy penalty relative to conventional processes without CO_2 capture [7]. This membrane-assisted CLR process could capture CO_2 at a negative cost due to the process intensification achieved (H_2 is produced directly from the membranes with no need for downstream processing units). However, H_2 membranes are still at an early stage of development and will require extensive testing in the hostile fluidized bed environment before this promising process can become commercially viable.

An important practical challenge faced by all chemical looping technologies is the scale-up of the interconnected reactor configuration under the pressurized conditions required for high process efficiency. Tightly controlled oxygen carrier circulation between the oxidation and reduction reactors is required to maintain overall mass and energy balances for achieving good fuel conversion. Oxygen carrier circulation is strongly influenced by the hydrodynamic behaviour of each fluidized bed reactor as well as the cyclones and loop seals between the reactors, requiring slow and careful scale-up of the technology. Pressurized operation significantly adds to this complexity.

Several reactor configurations have been proposed to address this challenge, including packed bed chemical looping [11], the rotating reactor [12] and gas switching technology [13]. This paper will focus on the gas switching technology where the oxygen carrier is kept in a single fluidized bed reactor and alternatively exposed to oxidizing and reducing gases. In this way, the cyclones and loop seals required to circulate the oxygen carrier material in chemical looping technology are replaced by simple inlet and outlet valves. More importantly, the reactor design is greatly simplified to a standalone bubbling fluidized bed, which can be easily scaled up and pressurized. Packed bed chemical looping offers similar advantages, but efficient operation is more challenging to achieve due to the complex interaction between the reaction and heat fronts moving through the reactor, which can cause high CH_4 slippage [14].

The gas switching reforming (GSR) process illustrated in Figure 1 will be the focus of this paper. In GSR, the reactor cycles through three steps: oxygen carrier reduction by PSA off-gas fuel, steam methane reforming, and oxidation with air. Due to the dynamic gas switching required in this process, a coordinated cluster of several standalone gas switching reactors is required to form a steady state processing unit [15]. Another important feature of GSR relative to CLR is that the reduction and reforming steps are inherently separated, allowing for efficient integration of the PSA off-gas fuel [16], which is important for maximizing efficiency. This advantage has also been identified by Spallina et al. [17] for hydrogen or methanol production using packed bed gas switching reforming reactors.

It is noted that the GSR reactor concept has been successfully demonstrated experimentally by Wassie et al. [18] where the reactor performance was studied as a function of reactor temperature and cycle length (degree of oxygen carrier utilization). Higher reactor temperature results in higher conversion of fuel and hence higher hydrogen yield, whereas longer cycle lengths (higher degree of oxygen carrier utilization) lowers the reactor temperature during the reforming step and hence reduces the fuel conversion.

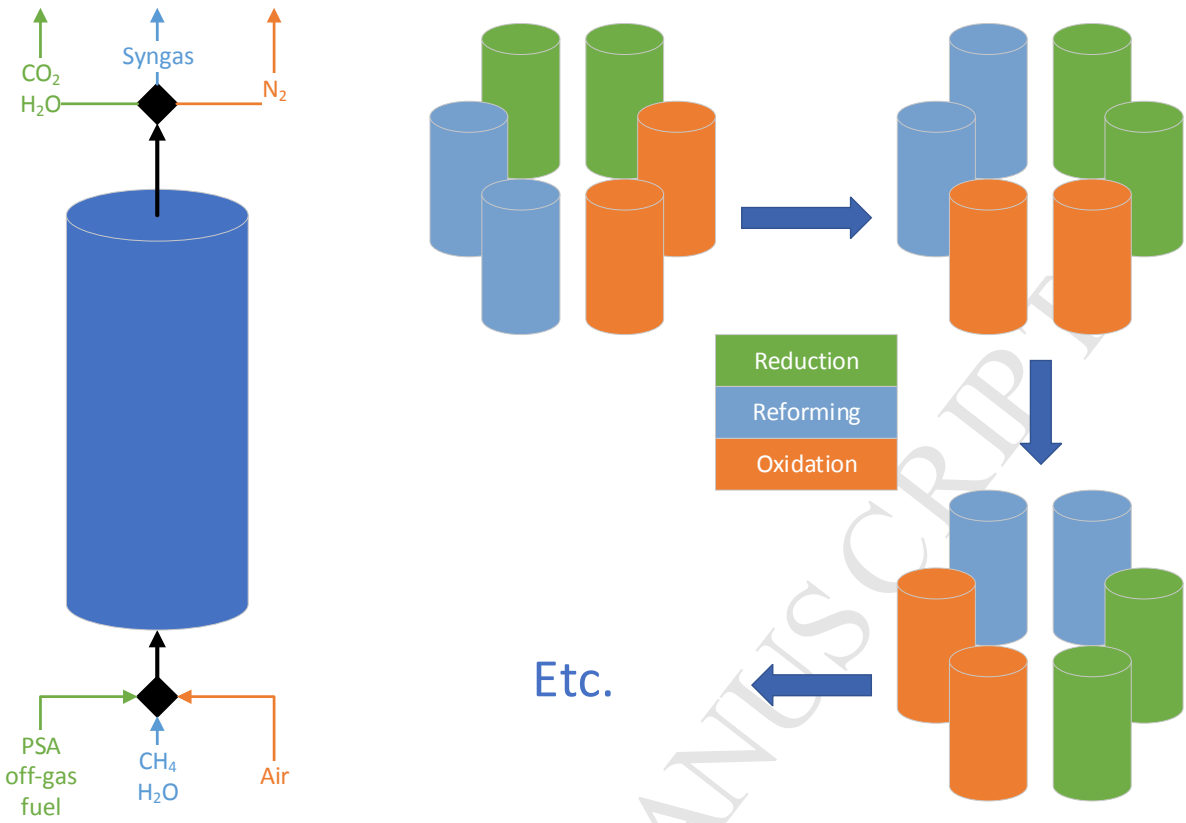

Figure 1: Left: The gas switching reforming reactor cycles through three steps: reduction, reforming and oxidation. Right: A cluster of gas switching reforming reactors operating as a steady state processing unit.

The objective of this paper is to present a first of its kind system level analysis of the GSR concept integrated into an H_2 production plant. The proposed process configuration, denoted as GSR-H2, is designed to mitigate typical challenges in hydrogen production with CO_2 capture such as:

- High efficiency penalty in the case of the conventional SMR plant with amine-absorption based CO_2 capture [7]. Aside from a small pressure drop, GSR imposes no energy penalty for CO_2 separation.
- A compromise between hydrogen purity and CO_2 stream purity in processes with membrane-assisted or sorption-enhanced water-gas shift and reforming [19]. The impure CO_2 stream from the PSA outlet can be efficiently combusted in the GSR reactors to yield good CO_2 purity in addition to high H_2 purity.
- Scalability of the chemical looping reforming process at higher pressures. The simple standalone bubbling fluidized bed reactors of GSR simplify design and scale-up [20].

A first of its kind techno-economic analysis of a GSR based combined cycle power plant, referred as GSR-CC, was presented by Nazir et al. [21]. The net electrical efficiency of the GSR-CC plant was estimated to be between 45.1% and 46.2%, which is ~12%-point less than the reference power plant without CO_2 capture. The economic analysis revealed that fuel and capital cost increases due to this relatively large energy penalty were the major drivers of the high CO_2 avoidance cost [21]. Further efforts to reduce the energy penalty resulted in a GSR-CC plant with efficiency penalty of 7.2%-points with respect to the reference power plant without CO_2 capture [22]. Furthermore, since the GSR-CC process can produce a 99.99% pure H_2 stream that is combusted in the gas turbine to produce power, it can be configured for

flexible electricity and pure H_2 production. Such a flexible plant offers attractive economic performance when balancing variable renewable energy [23].

The energy penalty in the GSR-CC process was primarily attributed to the need to generate steam for hydrogen production via steam methane reforming [22]. Since commercial H_2 production processes have similar steam requirements, it is expected that GSR will compare more favourably with benchmark technologies for hydrogen production than power production. In addition, the GSR process integration for H_2 production is simpler and would be implemented at a smaller scale than the integration for power production. For these reasons, hydrogen production is a more likely target for first deployment of the GSR technology. Previous GSR power plant studies were also limited to a GSR reactor pressure close to 18 bar for efficient integration with the power cycle operating at pressure ratios between 18-20 [21]. However, GSR for pure H_2 production does not face this limitation, allowing the pressure to be freely varied as an optimization parameter.

This work therefore presents a thorough assessment of the performance of the GSR-H2 plant over a range of design conditions relative to a reference SMR plant. GSR-H2 is also simulated without CO_2 capture to investigate the potential for early deployment of the technology before strong climate policies and CO_2 transport and storage infrastructure are in place. Following these results, clear conclusions regarding the potential of the GSR technology are presented and the requirements for future work are outlined.

2 Process description of reference SMR and GSR-H2 plant

2.1 Reference steam methane reforming plant without CO_2 capture

A steam methane reforming (SMR) plant with a fired tubular reformer (FTR) is considered as the reference plant for hydrogen production in this paper. The schematic of the process is shown in Figure 2 based on the process described before in Martinez et al. [24] and Spallina et al. [7]. The SMR plant is reproduced in this study to maintain consistency in the modelling assumptions across all the studied process cases. A typical natural gas (NG) input of 10 TPH is assumed as the basis for all the plants presented in this paper.

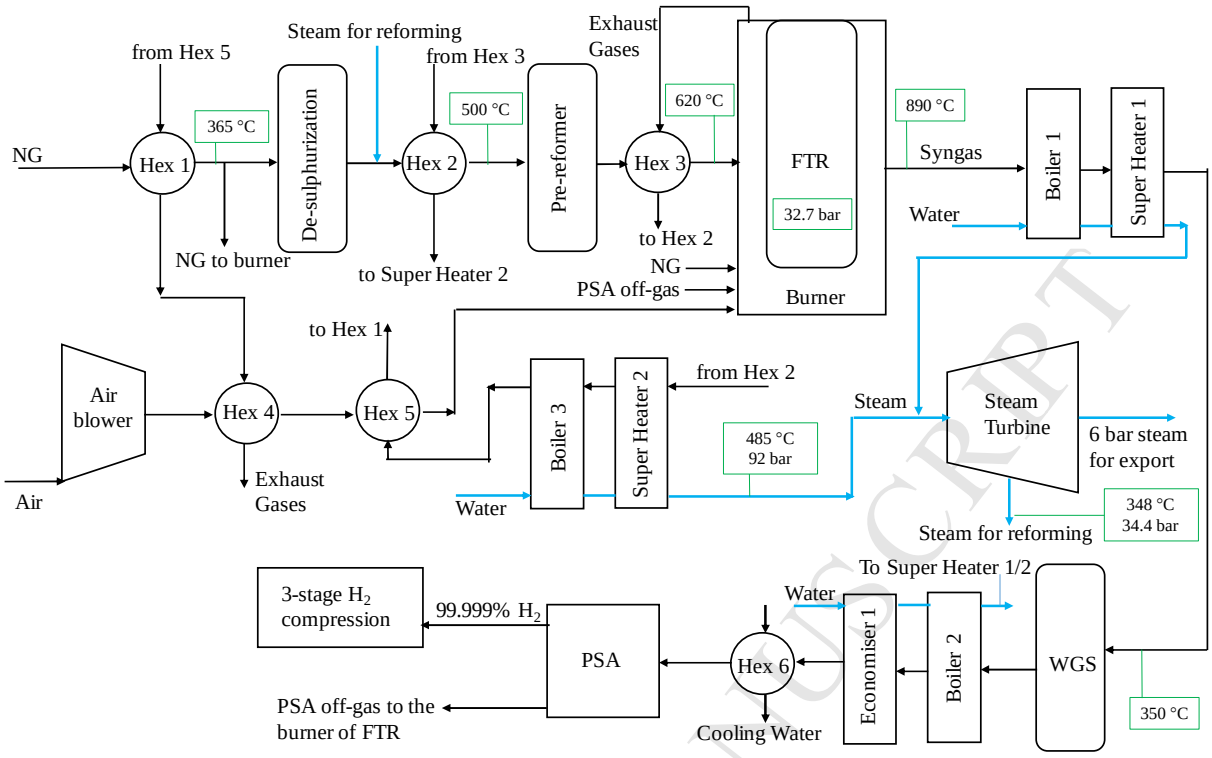

Figure 2: Schematic of the reference SMR plant that uses FTR for reforming without CO_2 capture.

NG is desulphurized, mixed with steam, pre-reformed to convert higher hydrocarbons and sent for reforming in the FTR at 32.7 bar with a S/C ratio of 2.7. The selection of the S/C ratio is based on industrial practices to avoid catalyst deactivation in the FTR [7]. A fraction of NG (3%) is extracted after the desulphurization step and combusted along with the off-gas from pressure swing adsorption (PSA) step in the burner of the FTR to provide the heat for the reforming reactions. Nearly 80% of the CH_4 is reformed in the FTR to form syngas, which is subsequently cooled and treated in the WGS reactor to convert the CO and H_2O into CO_2 and H_2, before 99.999% pure H_2 is recovered in the PSA. The pure H_2 is compressed and made ready for transport. Steam needed for reforming is prepared through heat recovery from the hot streams in the process. The excess steam produced is exported.

2.2 Hydrogen plant with gas switching reforming and CO_2 capture (GSR-H2)

The GSR-H2 process comprises of a cluster of GSR reactors for reforming NG, a WGS reactor, a PSA unit, and H_2 and CO_2 compression stages. It is similar to the conventional SMR process, where the GSR reforming step replaces the FTR tubes, while the oxidation and reduction steps replace the FTR furnace to achieve PSA off-gas combustion with integrated CO_2 capture. The pressurized operation of the combustion steps requires significant changes to the heat integration and energy recovery strategy compared to the reference plant.

A schematic of the base case GSR-H2 process is shown in Figure 3. NG is desulphurized, mixed with steam, pre-reformed to convert higher hydrocarbons and pre-heated before entering the GSR reforming step that is operated at 32.7 bar. The S/C ratio at the GSR inlet is 2.66, which is adjusted in every GSR-H2 simulation so that the PSA off-gas fuel (chemical potential energy not extracted as H_2 in the PSA) is just enough to supply the required amount

of heat to the reforming reaction. Steam needed for reforming is produced through heat recovery in a series of economisers and boilers as shown in Figure 3. NG is reformed with steam in the presence of the Ni catalyst to form syngas. The pre-heating of NG and the NG-steam mixture in Hex 1, 2 and 3 respectively is done by recovering heat from the hot syngas exiting the GSR reforming step. Similar to the reference plant, the syngas is treated in the WGS reactor to produce a stream containing mostly H_2 and CO_2, after which 99.999% pure H_2 is recovered in the PSA and compressed to 150 bar and 30 °C for export. The PSA off-gas is compressed, pre-heated and sent to the GSR reduction step. The reduction step outlet stream contains mostly CO_2 and H_2O, from which the H_2O is condensed, and the CO_2 stream is compressed for transport and storage. The reduced oxygen carrier is oxidized with compressed air during the oxidation step, leaving a hot stream containing mostly N_2. The N_2-stream is cooled and then expanded in a turbine before being vented.

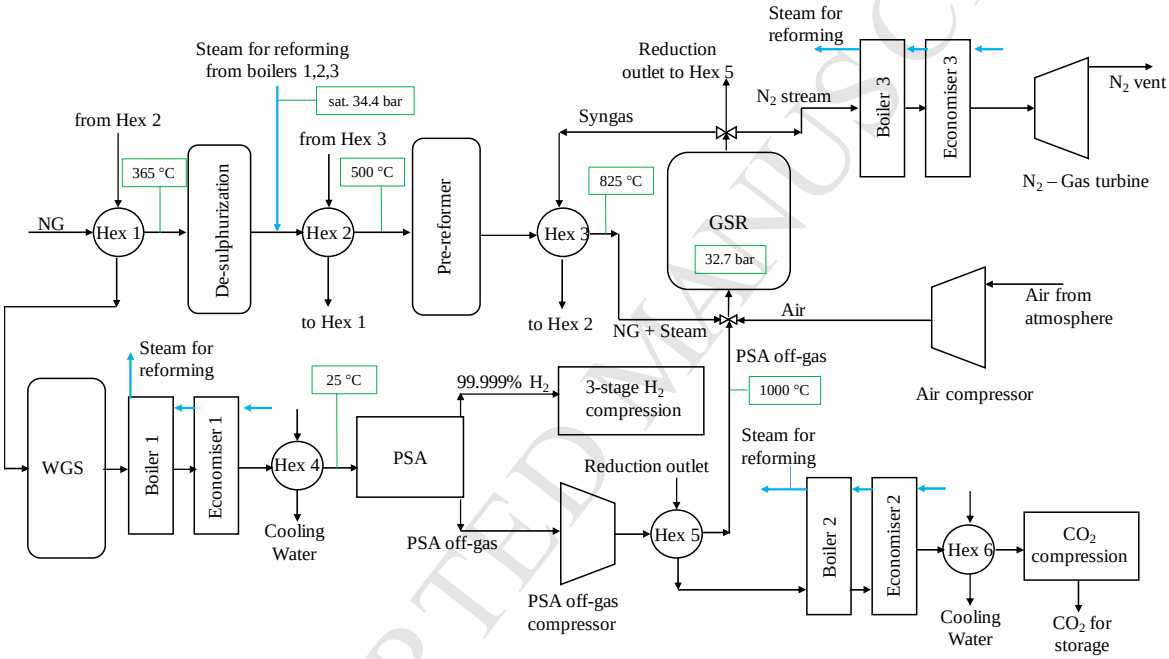

Figure 3: Schematic of the base case GSR-H2 plant that uses GSR for reforming (case $P_{32.7}$)

This paper aims to identify suitable GSR operating pressures for maximizing equivalent hydrogen production efficiency. Hence, the GSR-H2 process is designed and analysed for five different GSR operating pressures between 10 and 32.7 bar, i.e. 10 ,15, 20, 25 and 32.7 bar. Although most of the process remains the same as described above for the process operating at 32.7 bar, two important modifications are made for different GSR pressures. First, in the cases with 10-25 bar pressure, air for the GSR oxidation step is compressed in one stage since the final temperature of compressed air is within the limits of the compressor design (<500 °C). For the 32.7 bar case, air is compressed in two stages with intercooling. Second, in the cases with 10-25 bar pressure, Economiser 3 is shifted to after the N_2-gas turbine. Two factors are responsible for this change: 1) the turbine extracts less energy at low pressures, leaving more energy in the turbine outlet gases and 2) the S/C ratio for reforming becomes lower in the 20 and 25 bar cases, so more energy can be extracted in the form of work by the N_2-gas turbine instead of raising steam for reforming. The arrangement for the 32.7 bar case is as shown in Figure 3. Having higher pressures than 32.7 bar in the GSR reactor demands a

higher S/C ratio, for which steam needs to either be imported from a source outside the plant or produced on site by combusting additional fuel in a separate boiler.

As discussed in more detail in the subsequent reactor modelling section, the GSR-H2 process is also analysed with increased heat capacity inside the reactors by assuming added thermal mass in the form of metal rods that result in a doubling of the specific heat capacity. The main effect of this modification is that lower S/C ratios can be used to achieve the required level of methane conversion due to the higher average reforming temperature, thus requiring less energy for steam preparation. Four cases with 20, 25, 32.7 and 40 bar pressure were analysed for additional thermal mass in the GSR reactors. In this case, operation at 40 bar could be achieved without the need for steam imports or an additional boiler. Depending on the pressure, these cases also required some modifications to the N_2 stream treatment when compared to the GSR-H2 process described above. For the 20 bar case, both Boiler 3 and Economizer 3 were moved to after the N_2-gas turbine and additional heat was available for producing steam at 6 bar that is exported. For the 25 and 32.7 bar cases, the N_2 stream is expanded in the gas turbine, and the remaining heat in the turbine outlet gas is recovered to prepare saturated steam at 6 bar for export. In the 40 bar case, Boiler 3 is situated before the turbine and the remaining heat in the expanded N_2 stream is then recovered to prepare saturated steam at 6 bar for export. The definition of the cases analysed in this paper for different GSR pressures and additional thermal mass is shown in Table 1.

Table 1: Definition of different cases for pressure and additional thermal mass in the GSR

GSR Pressure	Additional thermal mass	Case definition
10	No	P_{10}
15	No	P_{15}
20	No	P_{20}
20	Yes	$P_{20\text{-}TH}$
25	No	P_{25}
25	Yes	$P_{25\text{-}TH}$
32.7	No	$P_{32.7}$ (base case GSR-H2)
32.7	Yes	$P_{32.7\text{-}TH}$
40	Yes	$P_{40\text{-}TH}$

3 Methodology and Assumptions

This section will be presented in two parts: reactor and process modelling. In the reactor modelling section, the methodology to obtain results from a 0D model of the GSR reactor is presented. The reactor modelling section describes the performance of the GSR reactor for the base case, i.e. when the GSR reactor is operated at 32.7 bar, both with and without additional thermal mass. The concentration and temperature profiles during each stage of the GSR process is shown for these cases. The results from the 0D model of the GSR are then used in the process model to carry out a system scale analysis of the GSR-H2 process and estimate the key performance indicators like equivalent hydrogen production efficiency, CO_2 capture and avoidance rate and specific primary energy consumption for CO_2 avoided (SPECCA). The process modelling section outlines the methodology and assumptions to model the GSR-H2 process followed by the equations to calculate the key performance indicators. A simple

model to estimate the recovery of 99.999% pure H_2 from the PSA system is also proposed based on the data points available in literature.

3.1 Reactor modelling

The transient behaviour of the GSR reactor is modelled in Matlab R2018b by solving the mass and energy balances of the reactor. This 0D model is based on two primary assumptions: 1) that the reactor behaves as a continuous stirred tank reactor (CSTR) and 2) that chemical and thermal equilibrium is reached within the reactor. Both these assumptions are reasonable considering the excellent mixing of fluidized beds and the large dimensions of industrial scale fluidized bed reactors. A previous experimental study showed that the highly reactive oxygen carrier employed in this work achieved equilibrium conversion even in a lab-scale reactor [18], adding further confidence in this assumption. More details regarding the balance and chemical reaction equations that are solved in the 0D model can be found in a previous study [21].

The only important modification in this study is that the percentage oxygen carrier utilization, i.e. the percentage of the 30 mass% active Ni in the oxygen carrier that is oxidized in the oxidation step, is set equal to the reactor pressure in bars. This is done to keep the undesired mixing when switching between the different reactor steps close to constant for the different reactor pressures considered in the present study, thus maintaining a similar level of CO_2 capture in all cases for ease of comparison.

Figure 4.a shows the general behaviour of the GSR reactor over a full cycle of operation in the base case. In the reduction step (0-1 on the x-axis), the fuel in the PSA off-gas reduces the oxygen carrier, yielding an outlet stream consisting mainly of CO_2 and H_2O. In the reforming step (1-4 on the x-axis), methane is reformed to hydrogen and carbon monoxide. The reactor temperature drops rapidly in this step due to the highly endothermic reforming reaction. Finally, in the oxidation step (4-5 on the x-axis), the oxygen carrier is oxidized by air, heating the reactor during the highly exothermic reaction. The undesired mixing of nitrogen into the reduction step and carbon dioxide into the oxidation step can also be observed.

Figure 4 shows the effect of reactor pressure on the GSR behaviour. Since the oxygen carrier utilization is kept proportional to the pressure, the step length increases with increasing reactor pressure. As a result, the temperature variation across the cycle is larger in Figure 4.a than in Figure 4.b. Since the maximum temperature in the cycle is maintained at 1100 °C, this leads to lower temperatures being reached in the higher pressure cases, which results in a lower average methane conversion across the entire reforming step. This is clearly visible in Figure 4, where the 32.7 bar case showed significant CH_4 slip towards the end of the reforming step, while CH_4 conversion in the 15 bar case is almost complete.

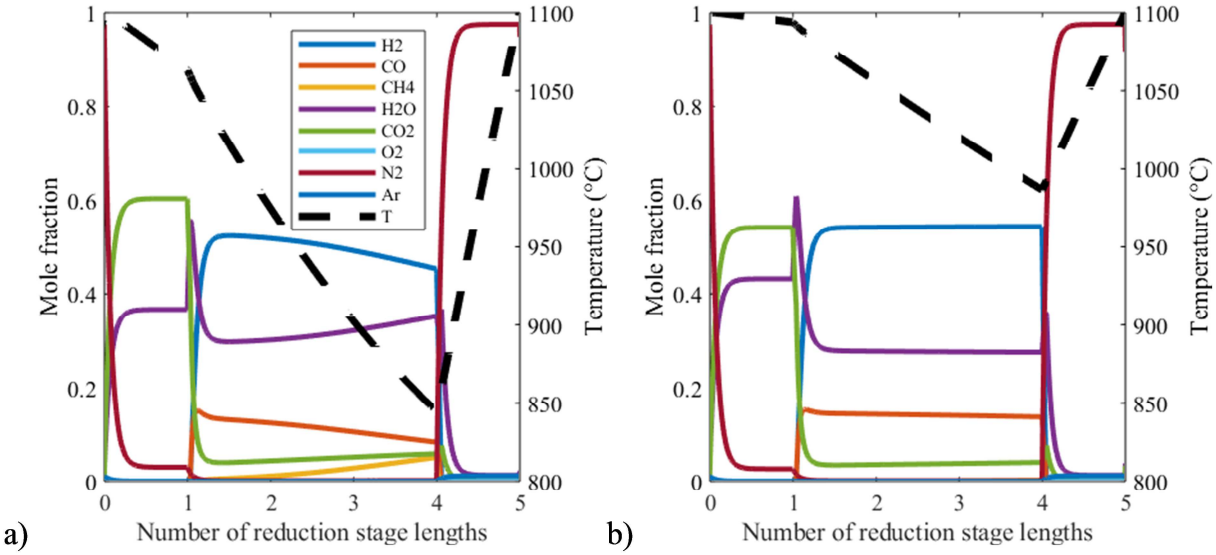

Figure 4: The temperature and composition as a function of the number of reduction step lengths for a full cycle of the GSR for a) a reactor pressure of 32.7 bar and b) a reactor pressure of 15 bar. The reduction step lengths are 401 s and 136 s respectively. Both cases are without added reactor thermal mass.

To counteract this challenge, additional cases were included where it was assumed that steel rods are inserted into the reactor such that the effective heat capacity of the oxygen carrier doubles. This will require about 25% of the reactor volume to be filled with steel rods and a 33% increase in total reactor volume to keep the active reactor volume constant. As shown in Figure 5, doubling the heat capacity in the reactor effectively halves the temperature variation throughout the cycle for the same oxygen carrier utilization. Consequently, the case with the added thermal mass leads to a significantly higher average temperature in the reforming step, resulting in a higher methane conversion. The lower S/C ratio used in the case with added thermal mass is also clearly visible in the stream compositions in Figure 5.b, showing lower H_2O and higher CO fractions in the reforming step.

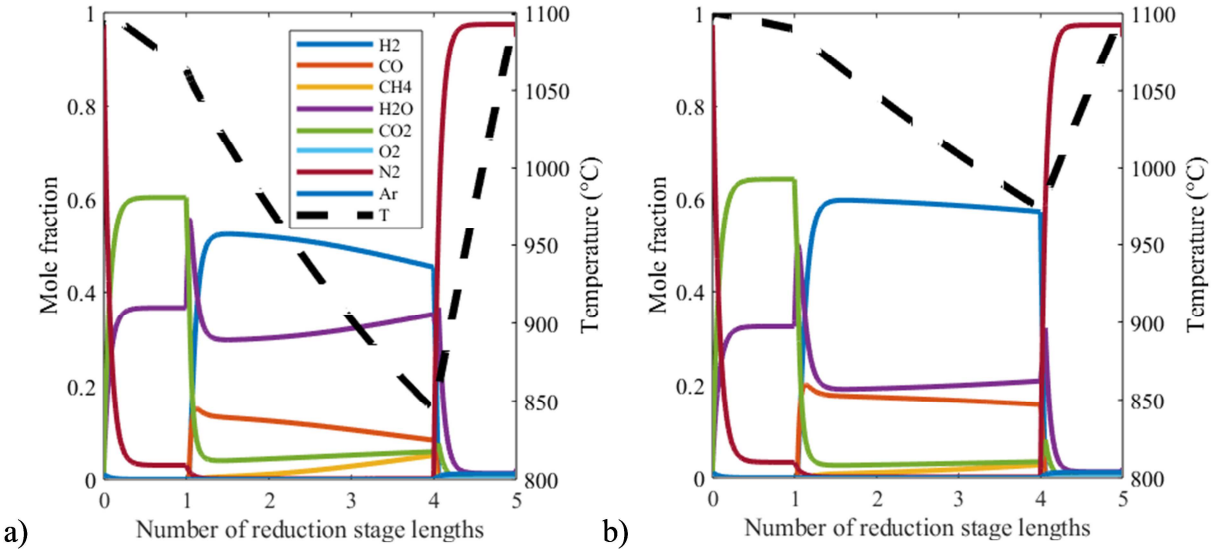

Figure 5: The temperature and composition as a function of the number of reduction step lengths for a full cycle of the GSR for a) without and b) with added reactor thermal mass. The reduction step lengths are 401 s and 315 s respectively. In both cases the reactor is operated at 32.7 bar.

3.2 Process modelling

All process components are modelled in Aspen Hysys V8.6 [25], except the GSR reactor, which is modelled in Matlab. The Peng-Robinson equation of state is used to estimate the thermodynamic properties of the components and the mixtures in the streams. A counter-current shell and tube configuration is assumed for the heat exchangers, boilers, economisers and superheaters. The pre-reformer and the FTR are modelled using the Gibbs reactor module and the WGS reactor using the equilibrium reactor module in Aspen Hysys, whereas the PSA is modelled as a black box with the H_2 recovery estimated from Eq. 1. Key process modelling assumptions are summarized in Table 2.

Table 2: Modelling assumptions employed in the SMR and GSR-H2 process simulations

Components	SMR plant	GSR-H2
NG conditions	• 70 bar and 15 °C • Mole composition: 89% methane, 7% ethane, 1% propane, 0.06% n-butane, 0.05% i-butane, 0.89% N_2, 2% CO_2	
Pressure drop in heat exchangers	• Gas side: 2% of the inlet pressure • Liquid side: 0.4 bar	
Polytropic efficiency of the air blower	80%	-
Polytropic efficiency of the air compressor	-	92.5%
Pressure drop in the pre-reformer and WGS reactor	1% of the inlet pressure	
Pressure drop in the reforming reactor	1% of the inlet pressure in the FTR	0.5 bar in the GSR
Pressure across the PSA	• H_2 stream pressure is 1% less than the inlet pressure	• H_2 stream pressure is 1% less than the inlet pressure

	• PSA off-gas is at 1.18 bar pressure	• PSA off-gas is at atmospheric pressure
Combustor pressure drop	1% of inlet pressure	-
Polytropic efficiency of hydrogen compressors	80%	
Polytropic efficiency of CO_2 compressor	-	80%
Polytropic efficiency of PSA off-gas compressor	-	80%
Adiabatic efficiency of the pumps	80%	
Fresh water conditions	15 °C at 1.01325 bar	
Cooling water conditions	17 °C at 2.92 bar (12 °C rise for cooling)	
Polytropic efficiency of steam turbine	80%	-
Polytropic efficiency of gas turbine (N_2-gas turbine)	-	92.5%
Minimum approach temperature in heat exchangers	• 20 °C for gas to gas • 10 °C for gas to liquid or liquid to gas	
CO_2 stream for transport and storage	-	• 25 °C • Final compression pressure (113-117 bar) dependent on the quality of the stream. The stream needs to be in liquid state.
H_2 stream for transport/storage	30 °C at 150 bar	
Exported steam conditions	6 bar and 165 °C	Saturated steam at 6 bar

The recovery of 99.999% pure H_2 is based on Eq. 1, where P_1 and P_2 are the pressures of the PSA feed and off-gas streams respectively. This equation is deduced from four data points [7, 26-28] that were available for high purity H_2 production from PSA in the literature. Although the equation does not capture the exact behaviour of the PSA unit, Figure 6 shows that it provides a reasonable estimate over the range of pressure ratios investigated in this study and that more detailed PSA modelling would only yield marginal increases in accuracy.

$$H_2\ recovery\ in\ PSA\ (\%) = 100 - \frac{100}{0.2521\left(\frac{P_1}{P_2}\right)+1.2706} \quad \textit{Eq. 1}$$

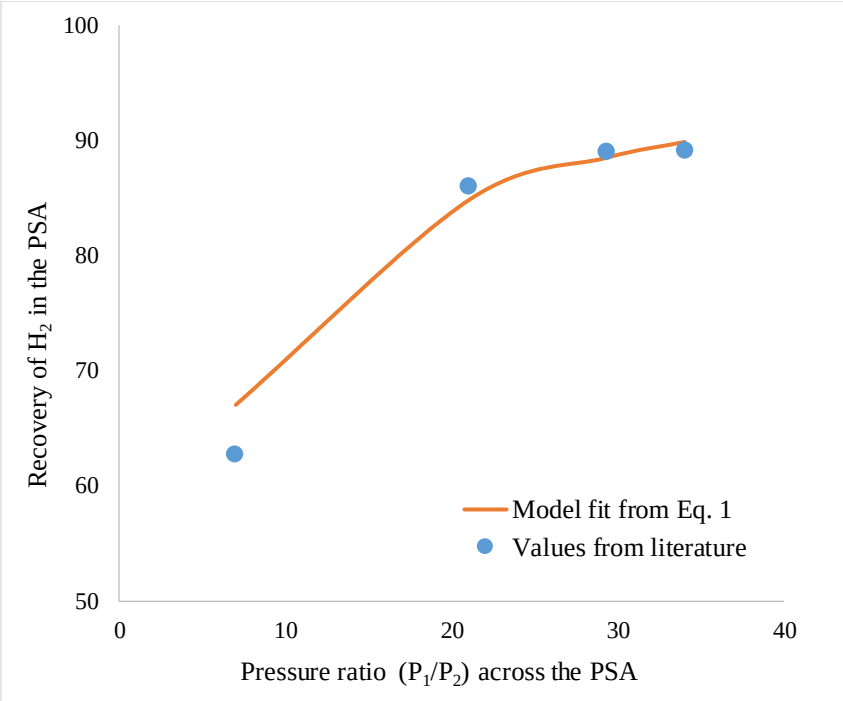

Figure 6: The match between Eq. 1 and the four datapoints from which it was derived to estimate hydrogen recovery around the PSA

Several performance indicators for the hydrogen production processes are defined below. Some indicators use the equivalent NG consumed in the process as given by Eq. 2, where W_{el} is the net electrical power production and Q_{th} is the thermal energy exports in the form of 6 bar saturated steam. The constants 0.9 and 0.583 are the efficiencies associated with using natural gas for steam generation in a boiler and power production in a combined cycle power plant respectively [7].

$$m_{eq,NG} = \dot{m}_{NG} \times LHV_{NG} - \frac{Q_{th}}{0.9} - \frac{W_{el}}{0.583} \quad \text{Eq. 2}$$

$$Q_{th} = \dot{m}_{steam\ export} \times (h_{steam@6bar} - h_{liqsat@6bar}) \quad \text{Eq. 3}$$

The hydrogen production efficiency and equivalent hydrogen production efficiency are defined as follows:

$$\eta_{H_2} = \frac{100\% \times \dot{m}_{H_2} \times LHV_{H_2}}{\dot{m}_{NG} \times LHV_{NG}} \quad \text{Eq. 4}$$

$$\eta_{eq,H_2} = \frac{100\% \times \dot{m}_{H_2} \times LHV_{H_2}}{\dot{m}_{eq,NG} \times LHV_{NG}} \quad \text{Eq. 5}$$

Next, the CO_2 capture and CO_2 avoidance are defined, where E_{NG} = 56.8 g_{CO_2}/MJ_{LHV} is the CO_2 intensity of natural gas combustion, whereas E_{th} = 63.3 g_{CO_2}/MJ and E_{el} = 97.7 g_{CO_2}/MJ are the avoided CO_2 intensities of steam and electricity exports respectively [7]. The values of E_{th} and E_{el} depend on the efficiency of converting natural gas to steam (0.9 in Eq. 2) and power (0.583 in Eq. 2).

$$CC = \frac{100\% \times mass\ of\ CO_2\ captured}{\dot{m}_{NG} \times LHV_{NG}} \quad \textit{Eq. 6}$$

$$CA = \frac{100\% \times mass\ of\ CO_2\ captured}{\dot{m}_{NG} \times LHV_{NG} \times E_{NG} - Q_{th} \times E_{th} - W_{el} \times E_{el}} \quad \textit{Eq. 7}$$

The process CO_2 intensity and its equivalent (g_{CO_2}/MJ) are expressed as follows:

$$E_{CO2} = \frac{mass\ of\ CO_2\ emitted}{\dot{m}_{H2} \times LHV_{H2}} \quad \textit{Eq. 8}$$

$$E_{eq,CO_2} = \frac{mass\ of\ CO_2\ emitted - Q_{th} \times E_{th} - W_{el} \times E_{el}}{\dot{m}_{H2} \times LHV_{H2}} \quad \textit{Eq. 9}$$

Finally, the specific energy consumption for CO_2 avoidance (MJ/kg_{CO_2}) is calculated according to Eq. 10.

$$SPECCA = 1000 \times \frac{\frac{1}{\eta_{eq,H2}} - \frac{1}{\eta_{eq,H2,ref}}}{E_{eq,CO2,ref} - E_{eq,CO2}} \quad \textit{Eq. 10}$$

4 Results and Discussion

The main results for the analysis for the SMR and GSR-H2 plants are shown in Table 3. Process performance for each case is quantified in terms of equivalent hydrogen production efficiency, CO_2 avoidance and SPECCA. The results for different cases are discussed below.

4.1 Reference SMR plant and base case GSR-H2 plant ($P_{32.7}$ case) analysis

The reference case SMR plant is simulated based on the plant described in Martinez et al. [24] and Spallina et al. [7]. The calculated equivalent hydrogen production efficiency is 79.28%, which is slightly below the 81-83% range in these studies [7, 24]. This difference is mainly attributable to differences in the PSA hydrogen recovery percentage, which is set to 86.57% in this paper (based on the Eq. 1) as opposed to 89% in the aforementioned works.

The base case GSR-H2 process (case $P_{32.7}$) shows an 8.1 %-point better hydrogen production efficiency than the reference SMR plant, but the equivalent hydrogen production efficiency is 3.8 %-points below the reference because of the high net electric power consumption of the GSR-H2 plant. The main efficiency penalty in the GSR-H2 plant with respect to the SMR plant comes from the air compressor, off-gas compressor and the CO_2 compression train, although some of this power consumption is cancelled out by the N_2-gas turbine. The SMR plant, on the other hand, has a steam turbine to expand the high-pressure steam (92 bar) produced through heat recovery in the process, with additional low-grade heat export in the form of 6 bar steam. As a result, the net electricity consumption in the reference SMR plant is 0.43 MW and 4.5 TPH of 6 bar steam is exported, whereas the base case GSR-H2 plant has a net electrical consumption of 10.56 MW with no steam export. It can be noted that the exported steam has a low economic value and, if the low-grade thermal energy in this stream is neglected in Eq. 2, the equivalent hydrogen production efficiency of the reference case drops to 77.48% (only 2 %-points higher than the GSR-H2 base case). When considering only

high-grade energy in the form of H_2 and electricity, the GSR-H2 plant produces 10.3 MW (LHV) more H_2 and consumes 10.1 MW more electricity than the SMR plant. It will therefore be more competitive in regions with access to low-cost electricity.

The base case GSR-H2 plant has a high CO_2 capture ratio of 96%, but a lower CO_2 avoidance of 84% because of the CO_2 emissions from the consumed electricity. The SPECCA for the base case GSR-H2 plant is 1.06 MJ/kg-CO_2. In summary, the base case GSR-H2 plant has an equivalent hydrogen production efficiency penalty of 3.8 %-points with 84% CO_2 avoidance relative to the reference SMR plant without CO_2 capture. This result compares favourably with conventional post-combustion CO_2 capture that shows an efficiency penalty of 14 %-points with 79% CO_2 avoidance [7].

Table 3: Main results for reference SMR plant and the GSR-H2 cases defined in Table 1

Cases	Units	SMR	GSR-H2 process								
			P_{10}	P_{15}	P_{20}	$P_{20\text{-TH}}$	P_{25}	$P_{25\text{-TH}}$	$P_{32.7}$ (Base case)	$P_{32.7\text{-TH}}$	$P_{40\text{-TH}}$
$m_{eq,NG}$ (Eq. 2**)**	TPH	9.83	11.46	11.27	11.14	10.75	11.19	10.76	11.40	10.76	10.87
Steam to Carbon ratio		2.70	2.99	2.51	2.11	1.95	2.14	1.82	2.66	1.80	1.92
H_2 produced	TPH	3.02	3.12	3.24	3.31	3.24	3.33	3.28	3.33	3.30	3.30
Hydrogen production efficiency (Eq. 4**)**	**%**	77.92	80.42	83.61	85.27	83.64	85.90	84.74	86.03	85.00	85.22
Equivalent H_2 production efficiency (Eq. 5**)**	**%**	79.28	70.17	74.22	76.54	77.83	76.76	78.79	75.45	79.01	78.37
Electricity Consumed											
Air compressor/blower	MW (MJ/kg-H_2)	0.33 (0.39)	4.36 (5.03)	5.09 (5.65)	5.63 (6.13)	5.86 (6.51)	6.11 (6.60)	6.37 (6.98)	6.78 (7.32)	6.98 (7.63)	7.22 (7.86)
H_2 compressors	MW (MJ/kg-H_2)	2.58 (3.08)	4.92 (5.68)	4.37 (4.85)	3.82 (4.16)	3.74 (4.16)	3.47 (3.75)	3.43 (3.75)	2.90 (3.13)	2.86 (3.13)	2.50 (2.73)
Pumps	MW (MJ/kg-H_2)	0.13 (0.15)	0.05 (0.06)	0.04 (0.05)	0.04 (0.05)	0.04 (0.04)	0.05 (0.05)	0.04 (0.04)	0.06 (0.07)	0.04 (0.05)	0.05 (0.06)
Off-gas compressor	MW (MJ/kg-H_2)		3.81 (4.40)	4.05 (4.50)	4.22 (4.59)	4.25 (4.72)	4.31 (4.66)	4.41 (4.83)	4.41 (4.76)	4.56 (4.98)	4.46 (4.86)
CO_2 compression	MW (MJ/kg-H_2)		1.98 (2.28)	1.53 (1.69)	1.22 (1.33)	1.26 (1.39)	1.01 (1.09)	1.04 (1.14)	0.87 (0.94)	0.81 (0.88)	0.64 (0.70)
Electricity Produced											
Steam Turbine	MW (MJ/kg-H_2)	2.61 (3.11)	-	-	-	-	-	-	-	-	-
N_2-gas turbine	MW (MJ/kg-H_2)		4.11 (4.74)	5.55 (6.17)	6.34 (6.91)	8.01 (8.90)	5.99 (6.47)	8.22 (9.00)	4.46 (4.82)	8.52 (9.31)	7.89 (8.60)
Net Electric Power	MW (MJ/kg-H_2)	-0.43 (-0.51)	-11.01 (-12.71)	-9.53 (-10.58)	-8.59 (-9.35)	-7.14 (-7.92)	-8.96 (-9.69)	-7.06 (-7.74)	-10.56 (-11.40)	-6.73 (-7.36)	-6.98 (-7.61)
Steam Exported (6 bar)	TPH	4.52	0.00	0.00	0.00	4.00	0.00	3.63	0.00	2.70	1.07
Q_{th} (Eq. 3**)**	MJ/hr	9592	0	0	0	8444	0	7653	0	5702	2246
Specific CO_2 emissions (Eq. 8**)**	g-CO_2/MJ	72.90	2.08	1.98	2.00	1.95	2.04	1.95	2.12	2.00	2.04
Equivalent CO_2 specific emissions (Eq. 9**)**	g-CO_2/MJ	71.64	12.44	10.60	9.62	7.03	9.93	7.02	11.40	7.07	7.87
SPECCA (Eq. 10**)**	MJ/kg-CO_2		2.77	1.41	0.73	0.36	0.67	0.12	1.06	0.07	0.23
CO_2 capture ratio (Eq. 6**)**	**%**		96.61	96.87	96.60	96.60	96.14	96.97	96.21	96.57	96.19
CO_2 avoidance (Eq. 7**)**	**%**		84.26	85.96	86.69	89.88	85.90	90.14	84.35	89.75	88.44

4.2 GSR-H2 process performance at different GSR operating pressures

The GSR operating pressure affects the performance of the GSR-H2 process in terms of the average temperatures in the different GSR steps and the energy recovery from the N_2 stream (Table 4). In general, higher reactor pressures require more oxygen carrier conversion in each step, leading to a lower average outlet temperature given the fixed maximum temperature of 1100 °C (see Figure 4). This reduction in average reactor temperature has an adverse effect on the equilibrium conversion of methane to syngas, which requires the use of a higher S/C ratio. The higher PSA efficiency at higher pressure ratios (Figure 6) offsets this effect to a certain degree because the process energy balance can facilitate lower CH_4 conversion if more of the converted fuel can be extracted as H_2. This trade-off results in a minimum S/C ratio in the 20-25 bar range (Table 3).

Table 4 indicates that this minimum S/C ratio corresponds with a minimum in WGS inlet temperature and air flowrate as well as a maximum in N_2-gas turbine inlet temperature. As shown in Figure 3, the steam required for the GSR-H2 process is produced by recovering heat from the shifted syngas from WGS, reduction outlet stream from Hex 5, and the N_2 stream from the GSR oxidation step. For high S/C ratios, the steam requirement is high and hence more heat is recovered from the N_2 stream resulting in lower N_2-gas turbine inlet temperatures. The work output from the turbine is a function of the TIT and the N_2 stream flow that is proportional to the airflow in the oxidation step of the GSR. Greater steam requirements also mean that more of the energy from the fuel must be converted to heat for raising steam. More fuel must therefore be combusted using oxygen from a larger air stream. The small reduction in WGS inlet temperature with lower S/C ratio is due to more cooling of the syngas stream in Hex 1 in Figure 3 if the stream contains less sensible heat from steam.

Table 4: Conditions in the GSR and the N_2-gas turbine for different pressure conditions in the GSR-H2 process

Cases	P_{10}	P_{15}	P_{20}	P_{25}	$P_{32.7}$
Steam to carbon (S/C) ratio	2.99	2.51	2.11	2.14	2.66
Reforming inlet Temperature (°C)	900	900	900	880	825
Syngas temperature (°C)	1059	1037	1012	985	939
WGS inlet temperature (°C)	316	311	296	291	302
Reduction step outlet temperature (°C)	1097	1097	1095	1090	1080
Oxidation step outlet temperature (°C)	1068	1050	1032	1014	990
TIT for N_2-gas turbine (°C)	507	720	827	743	456
Air flowrate to GSR (TPH)	52.8	49.0	46.6	45.3	45.5
Heat rejection to cooling water (MW)	21.62	16.95	14.10	13.48	14.77

Table 3 shows that H_2 compression work reduces at higher GSR operating pressures, since the H_2 stream exits the PSA unit at higher pressure. No significant difference is observed in the pump work for different cases. The PSA off-gas compressor work increases for higher GSR reactor pressures, whereas the CO_2 stream compression work reduces.

The hydrogen production efficiency of the GSR-H2 process increases with GSR operating pressure. The equivalent hydrogen production efficiency increases for design pressures between 10 and 25 bar, after which it starts decreasing again. This result indicates that minimization of the S/C ratio by optimizing the trade-off between the high GSR reforming temperature at low operating pressures and the high PSA efficiency at high operating pressures is the most important factor.

The most direct measure of the effect of S/C ratio on plant efficiency is the heat rejection from the low-temperature condensation of excess steam in Hex 4 and Hex 6 in Figure 3. As shown in Table 4, lower S/C ratios reduce the amount of heat rejection to cooling water, leaving more energy for recovery as H_2 from the PSA and electricity from the N_2-gas turbine.

For all the cases, the CO_2 capture and avoidance remain above 96% and 84% respectively. Hence, 25 bar is an optimum pressure in the GSR to produce hydrogen from the GSR-H2 process with higher efficiency and CO_2 capture. An economic assessment of the process, which is not in the scope of this study, will give more understanding in choosing the design pressure in the GSR. However, H_2 production from natural gas is sensitive to the fuel cost [7], implying that the most efficient plant will most likely be the most economical.

4.3 GSR-H2 process performance with added thermal mass in the reactors

The objective of adding more thermal mass inside the GSR reactor is to reduce the temperature drop during the endothermic reforming step so that the reforming is carried out at a higher temperature (see Figure 5). This allows the required degree of methane conversion to be achieved with lower S/C ratios. Figure 7 (a, b and c) shows that the temperatures of the GSR outlet streams increase significantly when additional thermal mass is assumed in the GSR reactors. This is due to the lower degree of temperature variation below the maximum temperature of 1100 °C in the GSR cycle.

In Figure 7 (e and g), it is noticeable that the reforming inlet and WGS inlet temperatures are higher for the cases with additional thermal mass. The temperature increase in these streams is caused by the higher syngas temperature at the GSR reforming step outlet (Figure 7.c) when additional thermal mass is included. A higher syngas temperature can achieve more fuel pre-heating in Hex 3 in Figure 3 and leaves more enthalpy in the stream exiting Hex 1 before the WGS reactors.

The GSR reforming inlet temperature was capped at 900 °C, resulting in a larger difference between reforming inlet and outlet temperatures in the cases with added thermal mass. This larger temperature difference requires slightly more fuel to be combusted to heat up the incoming gas streams. As a result, the air flow to the oxidation step of the GSR (Figure 7.d) is 3-5% higher for the cases with additional thermal mass to supply additional oxygen for fuel combustion, which is also reflected in the air compression work in Table 3.

As mentioned earlier, the main benefit of adding the thermal mass to the GSR reactors is a lower S/C ratio. Because of the lower S/C ratio, all the steam for reforming can be produced by heat recovery from shifted syngas after the WGS reactor and the reduction outlet stream from Hex 5 in Figure 3. Therefore, the hot N_2 stream from the GSR oxidation step can be directly expanded in the N_2-gas turbine to extract maximum work. It is seen in Figure 7.f that the TIT for the N_2-gas turbine is higher in the cases with added thermal

mass. The heat from the N_2 stream after expansion in the N_2-gas turbine is recovered to produce saturated 6 bar steam, which is exported.

The equivalent hydrogen production efficiency of the cases with added thermal mass (Figure 7.h) is higher than the cases without additional thermal mass. This is due to the lower steam requirement, which allows more of the energy in the N_2 stream from the GSR oxidation step to the converted to electricity instead of raising additional steam. Figure 7.h also shows that the optimum operating pressure for the GSR-H2 process is higher when additional thermal mass is included in the reactors. Case $P_{32.7\text{-}TH}$ has the highest equivalent hydrogen production efficiency of 79.01%, which is only 0.27%-points less than the reference case SMR plant without CO_2 capture. The SPECCA for the GSR-H2 process in case $P_{32.7\text{-}TH}$ is as low as 0.07 MJ/kg-CO_2, confirming that the GSR-H2 process has a high potential to efficiently produce hydrogen with nearly complete CO_2 capture. However, electricity imports remain significant and CO_2 avoidance is therefore dependent on the CO_2 emissions intensity of the imported electricity.

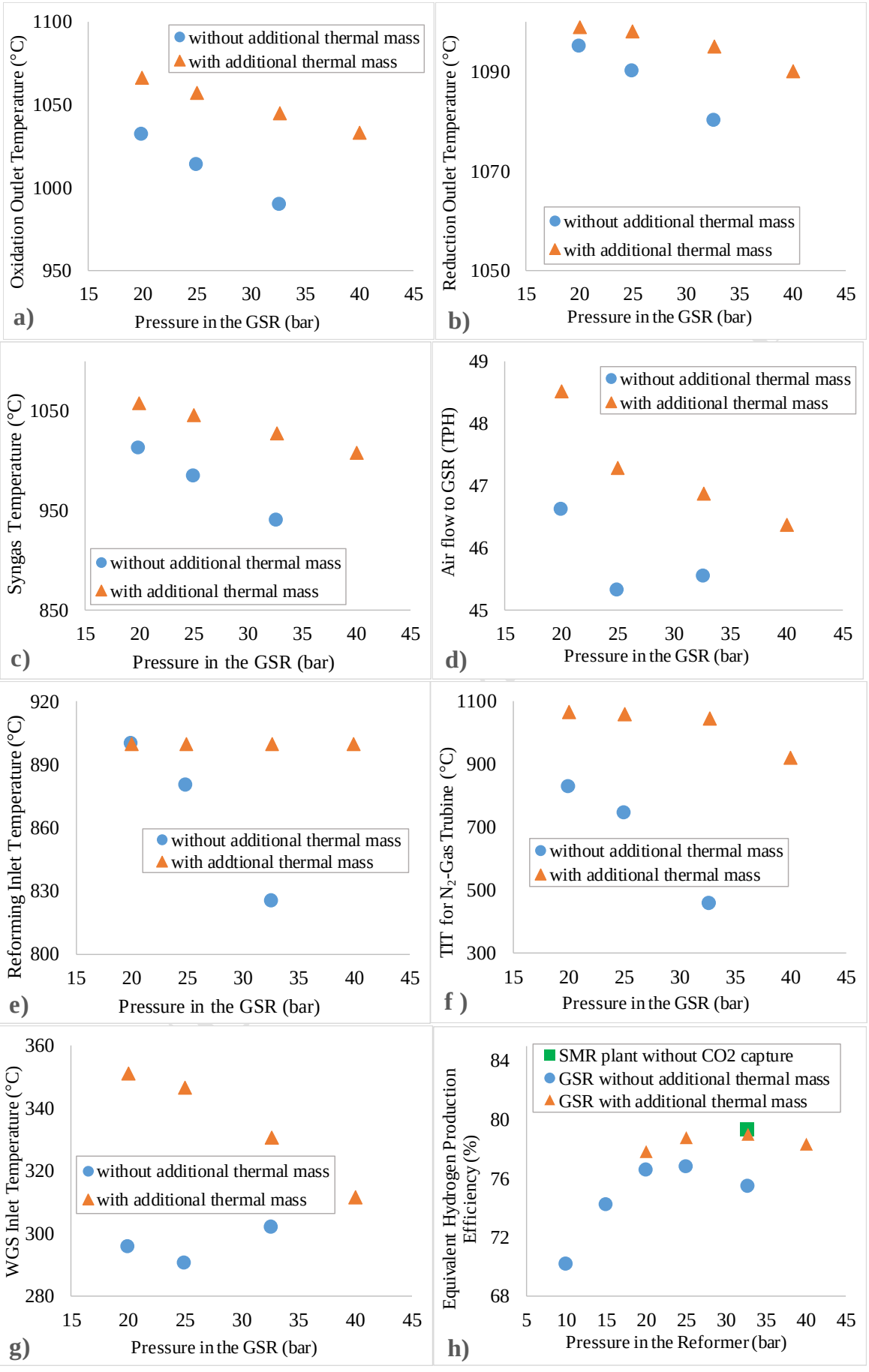
Oxidation Outlet Temperature (°C)
1100
1050
1000
950
without additional thermal mass
with additional thermal mass
15 20 25 30 35 40 45
Pressure in the GSR (bar)
a)
Reduction Outlet Temperature (°C)
1090
1070
1050
without additional thermal mass
with additional thermal mass
15 20 25 30 35 40 45
Pressure in the GSR (bar)
b)
Syngas Temperature (°C)
1050
950
850
without additional thermal mass
with additional thermal mass
15 20 25 30 35 40 45
Pressure in the GSR (bar)
c)
Air flow to GSR (TPH)
49
48
47
46
45
without additional thermal mass
with additional thermal mass
15 20 25 30 35 40 45
Pressure in the GSR (bar)
d)
Reforming Inlet Temperature (°C)
920
890
860
830
800
without additional thermal mass
with addtional thermal mass
15 20 25 30 35 40 45
Pressure in the GSR (bar)
e)
TIT for N2-Gas Trubine (°C)
1100
900
700
500
300
without additional thermal mass
with additional thermal mass
15 20 25 30 35 40 45
Pressure in the GSR (bar)
f)
WGS Inlet Temperature (°C)
360
340
320
300
280
without additional thermal mass
with additional thermal mass
15 20 25 30 35 40 45
Pressure in the GSR (bar)
g)
Equivalent Hydrogen Production Efficiency (%)
84
80
76
72
68
SMR plant without CO2 capture
GSR without additional thermal mass
GSR with additional thermal mass
5 10 15 20 25 30 35 40 45
Pressure in the Reformer (bar)
h)

Figure 7: Effect of additional thermal mass on conditions in the GSR-H2 process for different pressures in GSR

4.4 GSR-H2 without CO_2 capture

The equivalent hydrogen production efficiency of the GSR-H2 process without CO_2 capture is shown in Figure 8 for all the cases defined in Table 1. Instead of Hex 6 and the CO_2 compression step in Figure 3, a turbine is used to expand the CO_2 stream to produce additional power before venting to the atmosphere. Therefore, the overall power consumption in the GSR-H2 process is reduced and the equivalent hydrogen production efficiency increases by about 3 %-points. Figure 8 shows that the GSR-H2 process without CO_2 capture has higher equivalent hydrogen production efficiency than the SMR process for the cases with an operating pressure of 20 and 25 bar. All the cases with additional thermal mass in the GSR reactor have a higher equivalent hydrogen production efficiency than the SMR process.

The superior thermodynamic performance of the GSR concept relative to the conventional SMR plant is encouraging. Since efficiency has a large influence on process economics, it is possible that the GSR-H2 plant without capture can outcompete conventional H_2 production processes under current market conditions. In this case, GSR-H2 plants without CO_2 capture can be constructed independently of developments in climate policies. When CO_2 prices eventually increase strongly and CO_2 transport and storage infrastructure becomes available, the plant can easily be retrofitted for CO_2 capture by simply adding a CO_2 purification and compression train at a small efficiency penalty of around 3 %-points. In contrast, retrofitting conventional SMR plants with post combustion CO_2 capture will be a much more complex and expensive operation that results in an efficiency penalty of around 14 %-points [7]. Future economic assessment studies will investigate this possibility in detail.

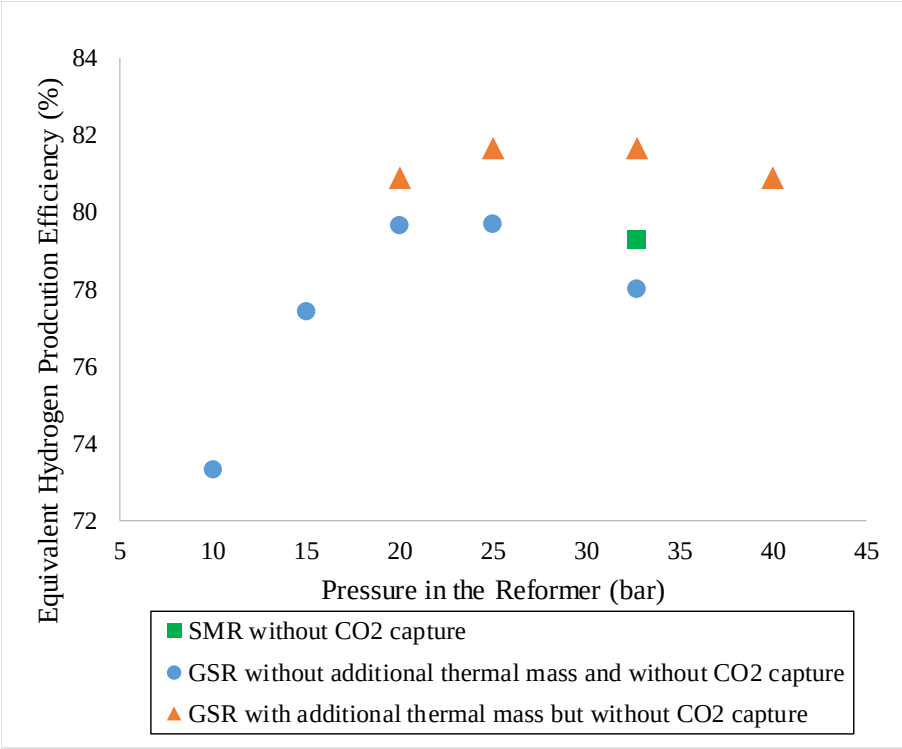

Figure 8: Equivalent hydrogen production efficiency of SMR and GSR-H2 process without CO_2 capture and compression for storage

4.5 Role of steam and electricity utilities

As seen in Table 3 and the discussion above, electricity consumption and steam exports significantly influence the equivalent hydrogen efficiency. In the cases presented above, electricity is imported from the grid where the conversion of natural gas to electricity is carried out in natural gas combined cycle (NGCC) plants. In addition, it is assumed that the excess steam produced from the process is exported for productive utilization in a facility nearby.

However, to make the hydrogen plant independent of the exports and imports in terms of steam and electricity, two scenarios are discussed for the cases defined in Table 5. All the GSR cases in Table 5 assume a GSR operating pressure equal to 32.7 bar. In scenario 1, the steam exports remain the same and are assumed to be exported to a facility nearby, whereas the net electrical efficiency of the power plant that provides the required electricity is varied between 20% to 70%. The change in power plant efficiency is reflected in Eq. 2, where the constant 0.583 (net electrical efficiency of a NGCC plant) is replaced with the respective net electrical efficiency. For example, the net electrical efficiency of a NG fired boiler integrated with a steam turbine is between 20-30%, whereas advanced combined cycles could have efficiencies in excess of 60%.

The change in the power plant efficiency also affects the CO_2 avoided and equivalent CO_2 emissions according to Eq. 11 and Eq. 12 respectively considering the term E_{el} changes according to (E_{NG}/power plant efficiency).

In scenario 2, the excess steam from the process (steam export) is expanded (to 0.05 bar) in a steam turbine (polytropic efficiency of 80%) on site, whereas the net electrical efficiency

of the power plant is varied between 20% and 70%. The main results for the two scenarios are discussed below.

Table 5: Definition of cases to study the scenarios for steam and electricity sources (GSR pressure = 32.7 bar)

Case	Definition
SMR	SMR plant without CO_2 capture
GSR-i	GSR-H2 plant without CO_2 capture and no additional thermal mass
GSR-ii	GSR-H2 plant with CO_2 capture and no additional thermal mass (case $P_{32.7}$ in Table 1)
GSR-iii	GSR-H2 plant without CO_2 capture and with additional thermal mass
GSR-iv	GSR-H2 plant with CO_2 capture and additional thermal mass (case $P_{32.7\text{-}TH}$ in Table 1)

4.5.1 Scenario 1: Steam is exported and electricity from a different source

As seen in Figure 9.a, the SMR plant is not sensitive to the power plant efficiency since the electricity requirements are small (Table 3). All the GSR plants are more sensitive to electricity conversion efficiency because of their substantial power consumption. If a NG boiler integrated with steam turbine is used onsite for electricity production (assuming the net electrical efficiency of it to be 30%), GSR-H2 plant with CO_2 capture (GSR-ii and GSR-iv) will have 5-11 %-point less equivalent hydrogen production efficiency than the SMR plant without capture. However, as seen in Figure 9.b, the CO_2 emissions will significantly reduce in the cases for GSR-H2 with CO_2 capture, although lower efficiency power cycles significantly increase equivalent emissions. Figure 9 also shows that GSR-H2 plant without CO_2 capture (GSR-iii) will outperform the SMR plant as long as the power plant efficiency is above 35%.

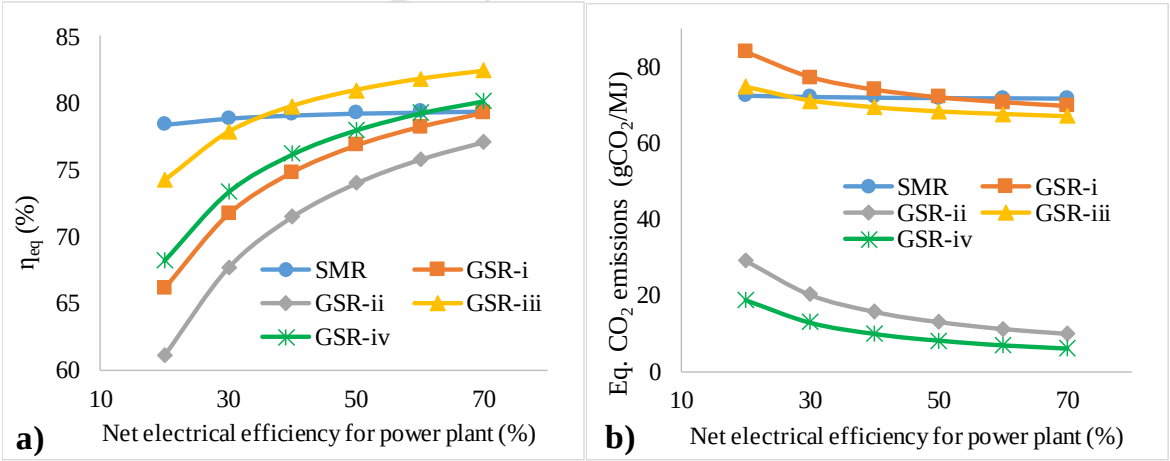

Figure 9: Results for scenario 1. a) Sensitivity of equivalent hydrogen production efficiency with the power plant efficiency b) Equivalent CO_2 emissions from the hydrogen plant at different power plant efficiencies

4.5.2 Scenario 2: Steam is expanded in turbine and electricity from a different source

Since the SMR plant exports the most steam, it will be most affected when steam exports are not possible, requiring on-site expansion to produce power at a low efficiency. In this scenario, the equivalent hydrogen production efficiency of the SMR plant is 2%-points less than the case where steam is exported. In contrast, the change in equivalent hydrogen production efficiency of the GSR-H2 process with and without CO_2 capture is less than 1%-points between scenario 1 and scenario 2 due to lower production of excess steam. As expected, Figure 10 shows similar trends to Figure 9, with the main difference being better performance of the GSR plants relative to the SMR benchmark. The equivalent CO_2 emission trends in scenario 2 (Figure 10.b) are slightly higher than observed in scenario 1, since the energy conversion factor to expand excess steam is less than using it for heating in a nearby facility.

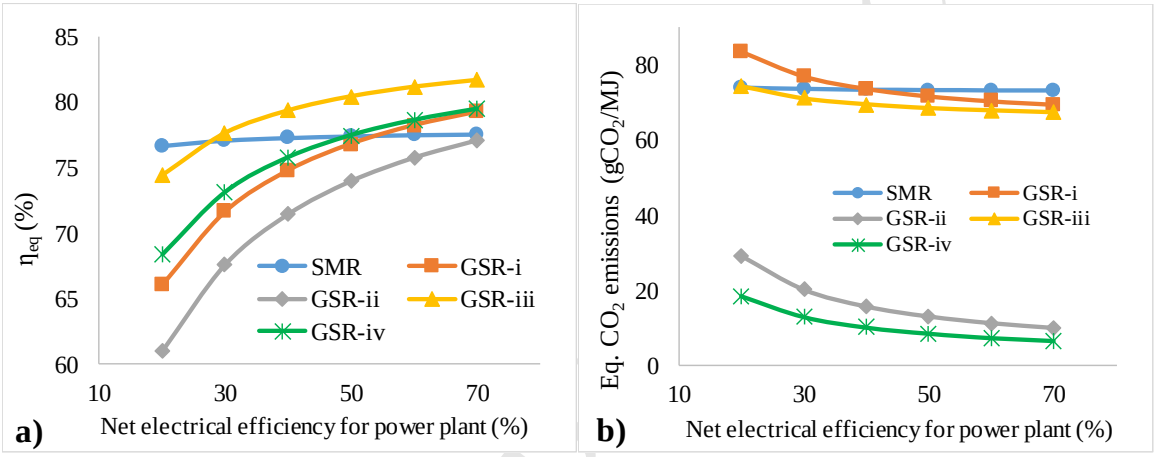

Figure 10: Results for scenario 2. a) Sensitivity of equivalent hydrogen production efficiency with the power plant efficiency b) Equivalent CO_2 emissions from the hydrogen plant at different power plant efficiencies

5 Conclusions

This study investigated the efficiency of the gas switching reforming (GSR) process for producing pure hydrogen with integrated CO_2 capture. GSR has high fundamental potential for efficient production of clean hydrogen because the heat for the endothermic steam methane reforming reaction can be produced by combusting the PSA off-gas fuel with inherent CO_2 capture without incurring a direct energy penalty.

The GSR operating pressure has an important effect on the GSR-H2 process. If the pressure becomes too low, the achievable H_2 separation efficiency in the PSA unit reduces substantially, thus lowering the overall process efficiency. On the other hand, excessively high pressures limit the methane conversion in the GSR reactors with the same negative effect on process efficiency. An intermediate pressure of 25 bar was found to be optimal in this case, returning an equivalent H_2 production efficiency that is 3.8 %-points lower than the reference SMR plant without CO_2 capture for a SPECCA of 0.67 MJ/kg-CO_2.

GSR-H2 process efficiency could be further improved by adding thermal mass to the reactors to reduce the amount of temperature variation across the transient GSR cycle. This allowed for higher reforming temperatures, in turn allowing for high methane conversion with lower S/C ratios. Lower steam requirements allowed more of the fuel energy to be converted to electricity instead of raising steam, thus increasing the equivalent H_2 production efficiency. As a result, the added thermal mass almost eliminated the energy penalty of the process with an insignificant SPECCA of 0.07 MJ/kg-CO_2.

The GSR-H2 process demands higher electricity imports when compared to the SMR plant, but is less dependent on steam exports. Therefore, GSR-H2 becomes less attractive when all power must be produced on site, but more attractive when steam exports are not possible. A fully independent plant that expands all excess steam in a steam turbine and produces all power requirements onsite with a thermal efficiency of 30% will increase the SPECCA of the GSR-H2 process to 1.15 MJ/kg-CO_2 and reduce the CO_2 avoided by 6 %-points.

When the CO_2 stream produced by the GSR-H_2 plant is expanded and vented instead of compressed for transport and storage, the hydrogen production efficiency increases by about 3 %-points, outperforming the reference SMR plant. Future work will investigate the economic performance of the GSR-H2 process with and without CO_2 capture to determine whether the attractive efficiencies translate into competitive H_2 production costs. In particular, the economic assessment will investigate an interesting business case where GSR-H_2 plants are constructed without CO_2 capture under current market conditions to be easily retrofitted for CO_2 capture with a minimal energy penalty when CO_2 prices eventually rise to high levels.

GSR-H2 is therefore seen as a promising method for clean H_2 production. The simple standalone bubbling fluidized bed GSR reactors are designed for easy operation under pressurized conditions, allowing for rapid scale-up. The primary technical uncertainty arises from the need for high temperature valves before and after the reactors for operation in the temperature range of 1000-1100 °C. In addition, the longevity of the proven and highly reactive oxygen carrier employed in this study should be thoroughly tested. Following these steps, the GSR-H2 process will be a viable candidate for producing clean hydrogen without a significant energy penalty relative to the benchmark process.

6 Acknowledgements

The current work is part of “GaSTech” project under the Horizon 2020 programme, ACT Grant Agreement No 691712. The authors appreciate the funding authorities, the Research Council of Norway and the European Commission. The authors also appreciate the project partners in GaSTech. The authors would also like to thank Dr. Luca Riboldi for sharing his understanding about the pressure swing adsorption systems.

References

[1] IPCC. Global Warming of 1.5 °C. Intergovernmental Panel on Climate Change; 2018.

[2] da Silva Veras T, Mozer TS, da Costa Rubim Messeder dos Santos D, da Silva César A. Hydrogen: Trends, production and characterization of the main process worldwide. International Journal of Hydrogen Energy. 2017;42(4):2018-33.

[3] Nikolaidis P, Poullikkas A. A comparative overview of hydrogen production processes. Renewable and Sustainable Energy Reviews. 2017;67:597-611.

[4] Dincer I, Acar C. Review and evaluation of hydrogen production methods for better sustainability. International Journal of Hydrogen Energy. 2015;40(34):11094-111.
[5] Khojasteh Salkuyeh Y, Saville BA, MacLean HL. Techno-economic analysis and life cycle assessment of hydrogen production from natural gas using current and emerging technologies. International Journal of Hydrogen Energy. 2017;42(30):18894-909.
[6] Collodi G. Hydrogen Production via Steam Reforming with CO2 Capture. Chemical Engineering Transactions. 2010;19:37-42.
[7] Spallina V, Pandolfo D, Battistella A, Romano MC, Van Sint Annaland M, Gallucci F. Techno-economic assessment of membrane assisted fluidized bed reactors for pure H2 production with CO2 capture. Energy Conversion and Management. 2016;120:257-73.
[8] Cormos A-M, Szima S, Fogarasi S, Cormos C-C. Economic Assessments of Hydrogen Production Processes Based on Natural Gas Reforming with Carbon Capture. CHEMICAL ENGINEERING TRANSACTIONS. 2018;70:1231-6.
[9] Rydén M, Lyngfelt A, Mattisson T. Synthesis gas generation by chemical-looping reforming in a continuously operating laboratory reactor. Fuel. 2006;85(12–13):1631-41.
[10] Nazir SM, Morgado JF, Bolland O, Quinta-Ferreira R, Amini S. Techno-economic assessment of chemical looping reforming of natural gas for hydrogen production and power generation with integrated CO2 capture. International Journal of Greenhouse Gas Control. 2018;78:7-20.
[11] Noorman S, van Sint Annaland M, Kuipers. Packed Bed Reactor Technology for Chemical-Looping Combustion. Industrial & Engineering Chemistry Research. 2007;46(12):4212-20.
[12] Håkonsen SF, Blom R. Chemical Looping Combustion in a Rotating Bed Reactor – Finding Optimal Process Conditions for Prototype Reactor. Environmental Science & Technology. 2011;45(22):9619-26.
[13] Zaabout A, Cloete S, Johansen ST, van Sint Annaland M, Gallucci F, Amini S. Experimental Demonstration of a Novel Gas Switching Combustion Reactor for Power Production with Integrated CO2 Capture. Industrial & Engineering Chemistry Research. 2013;52(39):14241-50.
[14] Diglio G, Bareschino P, Mancusi E, Pepe F. Simulation of hydrogen production through chemical looping reforming process in a packed-bed reactor. Chemical Engineering Research and Design. 2016;105:137-51.
[15] Cloete S, Romano MC, Chiesa P, Lozza G, Amini S. Integration of a Gas Switching Combustion (GSC) system in integrated gasification combined cycles. International Journal of Greenhouse Gas Control. 2015;42:340-56.
[16] Francisco Morgado J, Cloete S, Morud J, Gurker T, Amini S. Modelling study of two chemical looping reforming reactor configurations: looping vs. switching. Powder Technology. 2017;316(Supplement C):599-613.
[17] Spallina V, Marinello B, Gallucci F, Romano MC, Van Sint Annaland M. Chemical looping reforming in packed-bed reactors: Modelling, experimental validation and large-scale reactor design. Fuel Processing Technology. 2017;156:156-70.
[18] Wassie SA, Gallucci F, Zaabout A, Cloete S, Amini S, van Sint Annaland M. Hydrogen production with integrated CO2 capture in a novel gas switching reforming reactor: Proof-of-concept. International Journal of Hydrogen Energy. 2017;42(21):14367-79.
[19] Voldsund M, Jordal K, Anantharaman R. Hydrogen production with CO2 capture. International Journal of Hydrogen Energy. 2016;41(9):4969-92.
[20] Zaabout A, Dahl PI, Ugwu A, Tolchard JR, Cloete S, Amini S. Gas Switching Reforming (GSR) for syngas production with integrated CO2 capture using iron-based oxygen carriers. International Journal of Greenhouse Gas Control. 2019;81:170-80.
[21] Nazir SM, Cloete S, Bolland O, Amini S. Techno-economic assessment of the novel gas switching reforming (GSR) concept for gas-fired power production with integrated CO2 capture. International Journal of Hydrogen Energy. 2018;43(18):8754-69.
[22] Nazir SM, Cloete JH, Cloete S, Amini S. Gas switching reforming (GSR) for power generation with CO2 capture: Process efficiency improvement studies. Energy. 2019;167:757-65.
[23] Szima S, Nazir SM, Cloete S, Amini S, Fogarasi S, Cormos A-M, et al. Gas switching reforming for flexible power and hydrogen production to balance variable renewables. Renewable and Sustainable Energy Reviews. 2019;110:207-19.
[24] Martínez I, Romano MC, Chiesa P, Grasa G, Murillo R. Hydrogen production through sorption enhanced steam reforming of natural gas: Thermodynamic plant assessment. International Journal of Hydrogen Energy. 2013;38(35):15180-99.
[25] AspenHYSYS. Aspen HYSYS V8.6 User Guide. Aspen Technology Inc., Bedford, Massachusetts, USA; 2017.

[26] Riboldi L, Bolland O. Overview on Pressure Swing Adsorption (PSA) as CO2 Capture Technology: State-of-the-Art, Limits and Potentials. Energy Procedia. 2017;114(Supplement C):2390-400.
[27] Luberti M, Friedrich D, Brandani S, Ahn H. Design of a H2 PSA for cogeneration of ultrapure hydrogen and power at an advanced integrated gasification combined cycle with pre-combustion capture. Adsorption. 2014;20(2):511-24.
[28] Sircar S, Golden TC. Purification of Hydrogen by Pressure Swing Adsorption. Separation Science and Technology. 2000;35(5):667-87.

Highlights:

- Process design of the pure-H_2 production plant with CO_2 capture (GSR-H2) is presented
- Optimum design pressure for the gas switching reforming (GSR) reactor is identified
- GSR-H2 with 96% CO_2 capture shows only 3.8%-point efficiency penalty relative to conventional H_2 production process
- The efficiency penalty in GSR-H2 is eliminated by including additional thermal mass in the GSR reactor

AUTHOR DECLARATION

We wish to confirm that there are no known conflicts of interest associated with this publication and there has been no significant financial support for this work that could have influenced its outcome.

We confirm that the manuscript has been read and approved by all named authors and that there are no other persons who satisfied the criteria for authorship but are not listed. We further confirm that the order of authors listed in the manuscript has been approved by all of us.

We confirm that we have given due consideration to the protection of intellectual property associated with this work and that there are no impediments to publication, including the timing of publication, with respect to intellectual property. In so doing we confirm that we have followed the regulations of our institutions concerning intellectual property.

We further confirm that work covered in this manuscript does not involve either experimental animals or human patients.

We understand that the Corresponding Author is the sole contact for the Editorial process (including Editorial Manager and direct communications with the office). He is responsible for communicating with the other authors about progress, submissions of revisions and final approval of proofs. We confirm that we have provided a current, correct email address which is accessible by the Corresponding Author and which has been configured to accept email from (shareq.m.nazir@ntnu.no / mohdnazir.shareq@gmail.com)

Signed by all authors as follows: [LIST AUTHORS AND DATED SIGNATURES ALONGSIDE]

Shareq Mohd Nazir 26/05/2019

Jan Hendrik Cloete 26/0572019

Schalk Cloete 26/05/2019

Shahriar Amini 26/05/2019